International Journal of Mineral Processing and Extractive Metallurgy
2023; 8(1): 1-8
http://www.sciencepublishinggroup.com/j/ijmpem
doi: 10.11648/j.ijmpem.20230801.11
ISSN: 2575-1840 (Print); ISSN: 2575-1859 (Online)

Removal of Pb^{+2} and Cd^{+2} from Aqueous Solution by Using Faujasite

Fatma Mohamed Dardir[1, *], Ezzat Abdalla Ahmed[1], Mamdouh Farag Soliman[1], Mostafa Ragab Abukhadra[2]

[1]Geology Department, Faculty of Science, Assiut University, Asyut, Egypt

[2]Geology Department, Faculty of Science, Beni-Suef University, Beni Suef, Egypt

Email address:

fatmadardir@aun.edu.eg (Fatma Mohamed Dardir)

[*]Corresponding author

To cite this article:

Fatma Mohamed Dardir, Ezzat Abdalla Ahmed, Mamdouh Farag Soliman, Mostafa Ragab Abukhadra. Removal of Pb^{+2} and Cd^{+2} from Aqueous Solution by Using Faujasite. *International Journal of Mineral Processing and Extractive Metallurgy*. Vol. 8, No. 1, 2023, pp. 1-8. doi: 10.11648/j.ijmpem.20230801.11

Received: March 16, 2023; **Accepted**: April 7, 2023; **Published**: May 17, 2023

Abstract: The excess amount of lead (Pb^{+2}) and cadmium (Cd^{+2}) in the drinking water system lead to affect immunity and kidney failure problems. To overcome such troubles by developing well-crystalline faujasite minerals that are synthesized from claystone by the hydrothermal process may be the current trend For the effective adsorption of these cations. The active functional group, thermal nature, crystallinity surface, texture properties, and porous surface nature of faujasite were investigated using X-ray diffraction, scanning electron microscopy, Fourier-transform infrared, and nitrogen sorption 77k studies. The maximum removal of Pb^{+2} and Cd^{+2} was found to be 98% and 85% respectively using 60 mg and 70 mg from the adsorbent material. Moreover, the measured uptake capacity of Pb^{+2} and Cd^{+2} was 351.3 mg/g and 97.2 mg/g at equilibrium times of 50 min and 80 min respectively. Therefore, different adsorption isotherm and kinetic models were investigated. Accordingly, adsorption isotherms were the best fit for the Langmuir isotherm model. Moreover, the adsorption process for the two adsorbate cation was followed by the pseudo-second-order kinetics (R^2 >0.9), Elovich (R^2 >0.9 for Pb^{+2} and 0.86 for Cd^{+2}), and Langmuir (R^2 >0.9 for Pb^{+2} and 0.85 for Cd^{+2}). This indicates that the adsorption process via monolayer formation with chemical sharing or/and ion exchange process occurs on the energetically heterogeneous surface.

Keywords: Claystone, Faujasite, Adsorption, Lead, Cadmium, Kinetic, Isothermal Models

1. Introduction

Nowadays, industries, mining, printing and dyeing, and the chemical industry are increasing and spreading widely. Consequently, water pollution occurs with heavy metals, anions, oil, and organic materials resulting from the development and increase of these activities. So, water pollution became one of the most global environmental and health problems [1–4]. The most two common heavy metals that are dangerous are Pb^{+2} and Cd^{+2}, as their permissible concentration limits are 0.005 mg/L for Cd^{+2}, and 0.05 mg/L for Pb^{+2} according to US Environmental Protection Agency [5, 6], and increase in their limits leads to serious health problems. When lead ion concentrations increase than the permissible limit it will affect the digestive, nervous, immune systems, and brain [7, 8]. While the rise in the concentration of cadmium ions will cause damage to the bone and kidney and cause triggering some diseases emphysema and kidney damage [8–10].

There are many ways to remove heavy metals from polluted water, such as ion exchange [11–13], chemical precipitation [14–16], membrane filtration [17–19], and electrochemical treatment [20], etc but some of these methods are not common for separation processes as well as they have a high cost, limitations to reduce efficiency, production secondary sludge, and sensitive operating conditions. many comprehensive types of research are concerned with finding suitable high-efficiency adsorbents for the removal of hazard Pb (Ⅱ) and Cd (Ⅱ) from aqueous media. In the present days, available and low-cost several materials are used as an adsorbent for removing toxic metals

from wastewater such as clay [6, 21–23], zeolites [24–29], carbonaceous adsorbents [30–32], phosphates [2], and hydroxyapatite [8, 33].

In the present work, claystone was used as a raw material in the synthesis of faujasite because of its abundance and cheapness, unlike the use of natural zeolite, which is not available and its import is expensive. The raw materials are mixed with sodium hydroxide pellets with a specific ratio and through a hydrothermal process, the faujasite mineral was synthesized. Moreover, faujasite has a high surface area and high ion exchange so it is used as an adsorbent material for Pb and Cd ions from wastewater. The effect of faujasite dose, pH, time contact, and initial concentration were studied respectively. Also, the removal mechanism of the heavy metal ions and experimental aspects have been verified.

2. Materials and Methods

2.1. Materials

The raw sample was collected from Um El Huitat, Safaga area, Red Sea, Egypt. Sodium hydroxide NaOH 98% was a product of Aduic (Egypt. Pb and Cd nitrates were products of Sigma-Aldrich (Germany) that were used in the adsorption processes. Different concentrations were prepared from the pre-prepared standard stock solutions (1000 ppm). Sodium hydroxide (NaOH, 1M) and nitric acid (H_2SO_4, 1M) were used to control the solution pH.

2.2. Synthesis Steps

The first step in the synthesis of faujasite includes calcination of the raw sample at 900° c for 2 hours. Then, the calcined sample was mixed with sodium hydroxide pellets with a ratio of 1:1.2 and heated at 650° C for 2 hours. In the next step, 8.9 gm from the heated sample was mixed with 50 ml of distilled water and stirred for 4 hours. Subsequently, the sample was transferred into the Teflon tube and heated in the oven for 3 days at 80°c. Samples were washed several times with distilled water until the pH become 10 and then filtered. Finally, drying was effected at 60°c for 24 hours.

2.3. Characterization Techniques

To identify the mineralogical composition of raw and synthesized material we used an X-ray diffraction analysis. Diffraction patterns were obtained using an X-ray diffractometer (Model FW 1700 sieves, Phillips, Netherlands) with monochromatic Cuα radiation (λ= 1.540 A˚) employing a scanning rate of 0.06˚ min^{-1} and 2Θ rang 4 to 60˚ the diffraction data were analyzed using the DIFRAC plus evaluation package (EVA) software. SEM micrographs were obtained by a JEOL-JSM-5400 LV scanning electron microscope. FT-IR was recorded in 4000-400 cm-1 region with a Nicolled Spectrophotometer, model 6700 (USA) in the attenuated total reflectance (ATR) mode. The S_{BET} values were estimated based on Brunauer–Emmett–Teller (BET) method from N_2 adsorption at 77K.

2.4. Adsorption Studies

The removal of heavy metals by using faujasite as an adsorbent was studied under the effect of many impacts viz, the effect of adsorbent dose in the range (10-70 mg), at pH 6, at 120 min, and at 800 ppm for Pb while 200 ppm in case of Cd. Moreover, the effect of solution PH range from 2 up to 9 at 120 mints, 50 mg dose of adsorbent, and at 800, and 200 ppm concentration of Pb and Cd respectively. Also, the effect of contact time under the same conditions is considered above. Finally, the impact of adsorbate concentration was studied in the range of 50 to 1200 ppm for Pb^{+2} while in the case of Cd^{+2}, the range was 50 to 500 ppm on the whole the appropriate isothermal models for adsorption were inspected at constant and under different conditions.

3. Results and Discussion

3.1. Characterization

3.1.1. X-ray Diffraction (XRD)

X-ray results of the raw material that was used in the synthesis of zeolites show that it is composed of smectite and quartz Figure 1, while the X-ray diffractogram of the synthesized material illustrates that the product material is a faujasite mineral which matched beautifully with the standard ASTM cards. The main peak appears at 2Θ = 6 [34, 35] Figure 2.

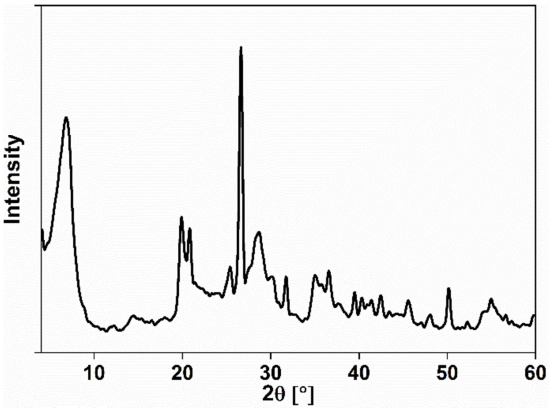

Figure 1. *XRD for the precursor raw sample.*

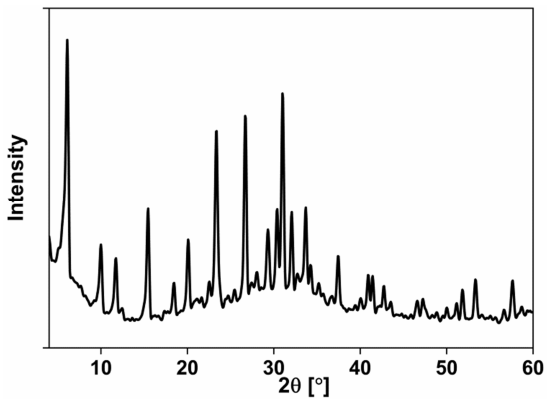

Figure 2. *XRD for the synthesized zeolite mineral.*

3.1.2. Scanning Electron Microscope (SEM)

A scanning electron microscope (SEM) image of the synthesized mineral is presented in Figure 3. It was shown that it is composed of nanocrystal aggregates from octahedral [24, 25, 28].

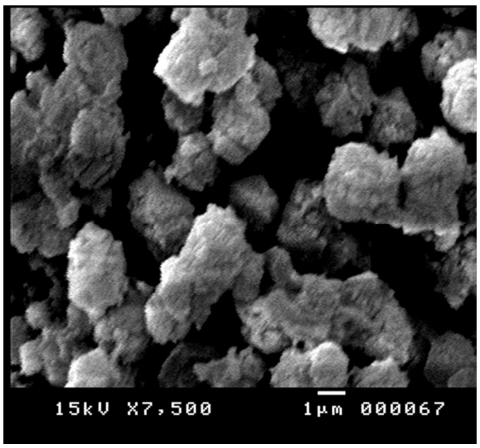

Figure 3. *SEM image shows nanocrystal aggregates of faujasite.*

3.1.3. Fourier Transform Infrared (FT-IR)

The FT-IR spectrum of the synthesized sample under investigation was given in Figure 4. Examining the spectrogram one can observe the following characteristic bands located at 3477, 1634, 1465, 984, 754, 675, 563, and 462 cm^{-1} bands. The band observed at 3477 cm^{-1} is attributed to the O-H vibration. While the band appeared at 1634 cm^{-1} due to bending mode. The bands located at 1465 and 984 cm^{-1} are attributed to the external T-O-T (T= Si and/or Al) asymmetric starching and the internal asymmetrical one respectively. On the other hand, the bands presented at 754 and 675 cm^{-1} correspond to the external and internal symmetric vibration respectively. Furthermore, the double ring vibration belongs to the band O-T-O which is located at 563 cm^{-1}. The band at 462 cm^{-1} is attributed to bending vibration [26, 27, 29, 36].

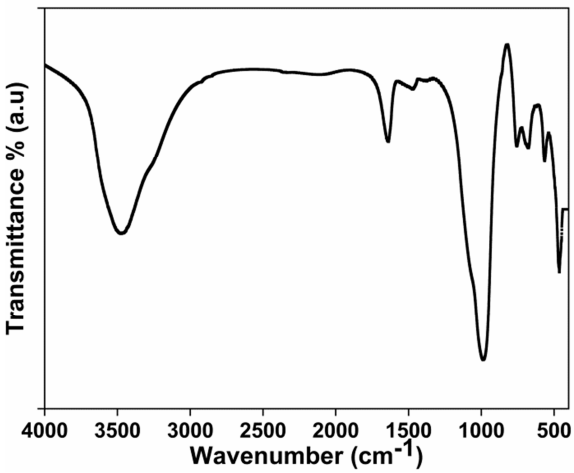

Figure 4. *FT-IR of the synthesized faujasite mineral.*

3.1.4. Surface Area Mesurements

The surface area of faujasite was measured using Brunauer–Emmett–Teller method. The synthesized product has a high surface area which is found to be 247 m^2/g.

3.2. Adsorption Results

3.2.1. Effect of Adsorbent Dose

The relationship between the adsorbent dose and removal percentage of Pb^{+2} and Cd^{+2} was illustrated in Figure 5. The removal percentage of Pb^{+2} and Cd^{+2} increases upon increasing the adsorbent dose. The maximum removal of Pb^{+2} is 98% using an adsorbent dose of 60 mg while the maximum removal of Cd^{+2} is 85% by dealing with a 70 mg adsorbent dose. These higher values of cations removal may be attributed to both large surface area and available excess active adsorption sites located at the surface of the adsorbent [8, 37].

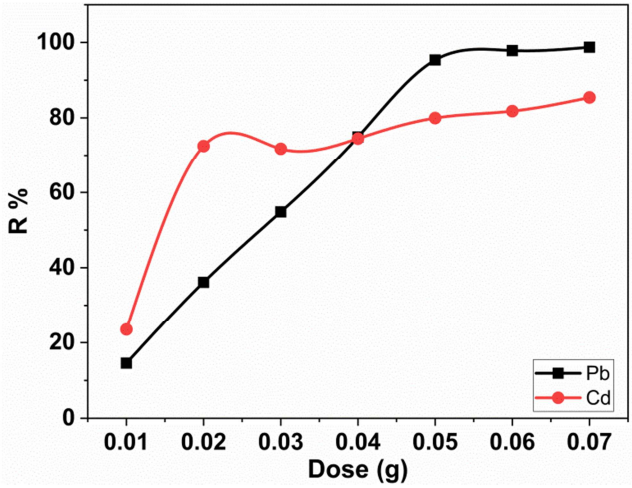

Figure 5. *The relation between adsorbent dose and removal of Pb^{+2} and Cd^{+2}.*

3.2.2. Effect of Solution pH

The effect of solution pH (2-9) in the removal process of heavy metals by the action of faujasite as an adsorbent was studied as one of many parameters that affect both the adsorption capacity and its mechanism [38, 39]. Concerning Cd^{2+} ions, the nature of the adsorptive species depends mainly on the pH value. In the range from 2 to 8 Cd^{+2} ions exist either free cations or aqueous ones $[Cd(H_2O_6)]^{2+}$ were at pH >8 the hydroxo complexes $[Cd(OH)]^{+}$ is dominated [40]. In the case of Pb^{2+} at a pH value above 5, the hydroxide species which have the general formula $([Pb(OH)_n]^{2-n}$, where n= 1,2, and 4 were detected [41]. Taking into consideration that the zeolite surface is positively charged, if we are dealing with acidic conditions, it will stimulate more strong attractive anions whereas, in the basic medium, the attractiveness is directed towards the cationic metals [6, 33, 42, 43]. Figure 6 shows the removal percentage of Pb^{+2} and Cd^{+2} as a function of pH. The results illustrated that the removal percentage increased with the increasing PH of the solution. The maximum removal of Pb^{+2} was achieved at a low pH value of 4 but the removal of Cd^{+2} reached its maximum at a pH value of 5.

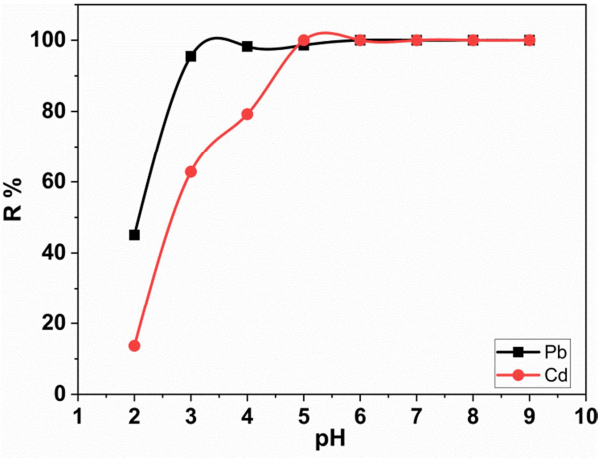

Figure 6. *The relationship between solution pH and removal percentage of Pb^{+2} and Cd^{+2}.*

3.2.3. Effect of Contact Time and Kinetic Models

The contact time plays an important role in the adsorption properties of zeolite minerals. The effect of contact time is illustrated graphically in Figures 7 a and b. the plots show that the adsorption capacity varies and exhibits two different stages. The first stage is characterized by a rapid increase in adsorption capacity with increasing time until we reach equilibrium time. In the second stage, the adsorption capacity reflects slight increases or is nearly constant. After equilibrium is reached the adsorption capacity decreases slightly over time, giving a plateau with nearly constant capacities. This behavior is due to the availability of active sites on the surface of the adsorbent material that is being reduced with increasing contact time [44, 45].

The adsorption capacity of Pb^{+2} in the first stage increases within the range from 17.5 to 351.3 mg/g with increasing time from 0 to 50 mins while the equilibrium stage was attended at 50 mins Figure 7a. Figure 7b shows the behavior of Cd^{+2} where the initial stage was terminated at 80 mins which belongs to 97.2 mg/g.

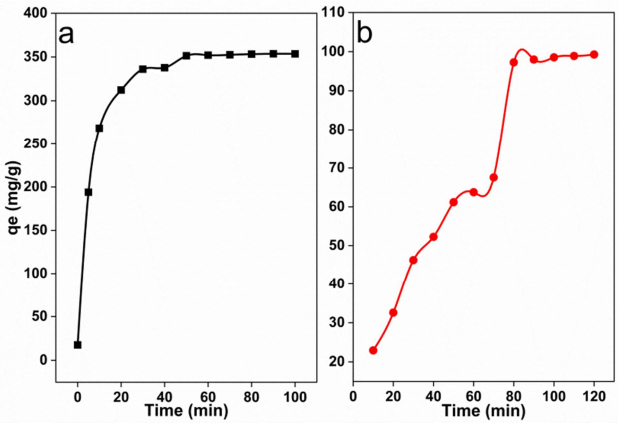

Figure 7. *The effect of contact time (a) for Pb^{+2} and (b) for Cd^{+2}.*

Concerning kinetic models, there are three models were applied to describe the adsorption mechanism. The first model is the pseudo-second-order, which was applied to justify that the adsorption processes proceed by chemical sorption through ions sharing and/or sharing between soluble ions and adsorbent [44, 46]. The linear fitting of this model is shown by equation (1). The parameters given in the equation were calculated and presented in Table 1.

$$t/q_t = 1/k_2 q_e^2 + t/q_e \quad (1)$$

where q_t is the amount of cation adsorbed at time t (mg/g) and k_2 is the reaction rate constant (g/mg min). Figure 8 shows a higher and better fitting upon applying this model. The quantity of experimental adsorption capacity results matches very well with the theoretical one.

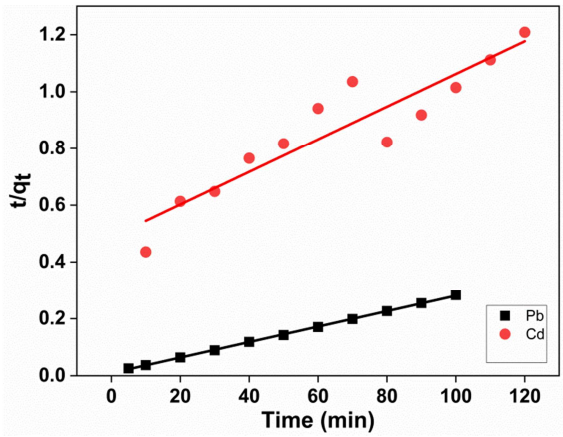

Figure 8. *Pseudo-second order for Pb^{+2} and Cd^{+2}.*

The second model is the Elovich model This model has been applied as a mass transfer model for heterogeneous diffusion [47]. The linear fitting of this model is expressed in Eq. (2).

$$q_t = \frac{1}{\beta} ln(\alpha\beta) + \frac{1}{\beta} ln(t) \quad (2)$$

where β parameter represents the degree of activation energy, desorption coefficient sand surface coverage (g/mg) and α parameter is the initial uptake rate (mg/mg.min) at reaction time t = 0min. the linear fitting of this model is presented graphically in Figure 9 and these parameters are estimated and listed in Table 1. All data possess a reasonable fit with a correlation coefficient $R^2 > 0.9$.

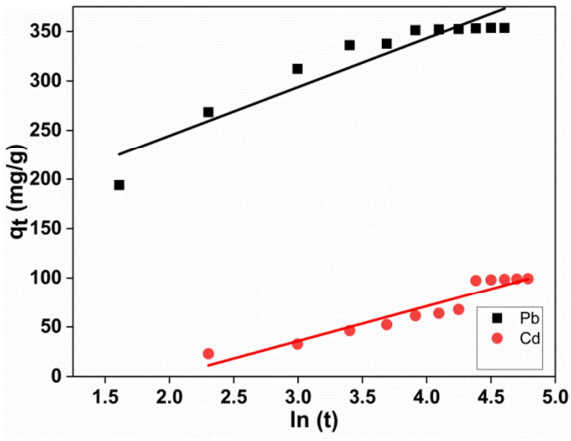

Figure 9. *Elovich kinetic model for Pb^{+2} and Cd^{+2}.*

The last model that is used in this study is intra-particle diffusion. It is known that this model describes the transfer of the dissolved ions from the bulk of the solution to the adsorbent solid surface followed by the intra-particle transport/ diffusion process [2, 48]. Moreover, it is shown in equation (3).

$$q_t = k_p t^{1/2} + C \quad (3)$$

The intercept related to the thickness of the boundary layer and k_p is the internal-particle diffusion constant (mg g^{-1} min^{-1}). The adsorption results and their fitting with the model are represented graphically in Figure 10. Each adsorption curve is dispersed into two stages the first one is related to the adsorption of heavy metal ions on the surface of the adsorbent indicating the effect of the boundary layer while the second stage in the presented curves is related to the adsorption of heavy metals onto the pores sites. Accordingly, one can conclude that the adsorption of heavy metal ions was adsorbed not only at the surface but also by the pore diffusion mechanism [49, 50].

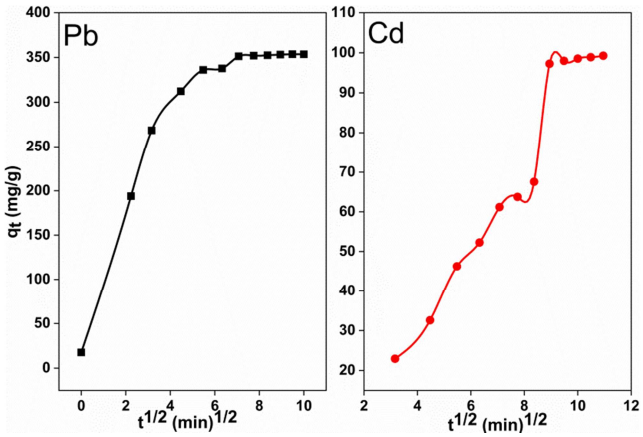

Figure 10. *Intra-particle diffusion model for Pb^{+2} and Cd^{+2}.*

Table 1. *The calculated parameters of kinetic models.*

	parameters	Faujasite	
		Pb^{+2}	Cd^{+2}
Pseudo-second order	qe (mg/g)	370	185
	k_2 (mg/min)	$7x10^{-4}$	$5.9x10^{-5}$
	R^2	0.99	0.86
Elovich	β (g/mg)	0.0144	0.0283
	α (mg/g min)	186.947	4.8448
	R^2	0.91	0.9

3.2.4. Equilibrium Studies and Isothermal Models

The initial concentration of Pb^{+2} and Cd^{+2} ions was studied as a parameter that affects the adsorption behavior of faujasite adsorbent. The concentration range in this study of Pb^{+2} started from 50 mg/L to 1200 mg/L whereas the range in the case of Cd^{+2} begins from 50 mg/L to 500 mg/L. The relation between adsorption capacity and the initial concentration of Pb^{+2} and Cd^{+2} is shown in Figure 11. The obtained results illustrate that the capacity uptake of Pb^{+2} ions increases from 24 to 375 mg/g with increasing the initial concentration from 50 mg/L to 800 mg/L respectively until reaching equilibrium at a value starting from 800 mg/L after which the capacity is fixed or slightly increases. On the other hand, the uptake capacity of Cd^{+2} increases from 14 mg/g to 75 mg/g with increasing the initial concentration from 50 mg/L to 350 mg/L then the equilibrium was attained at such capacity value.

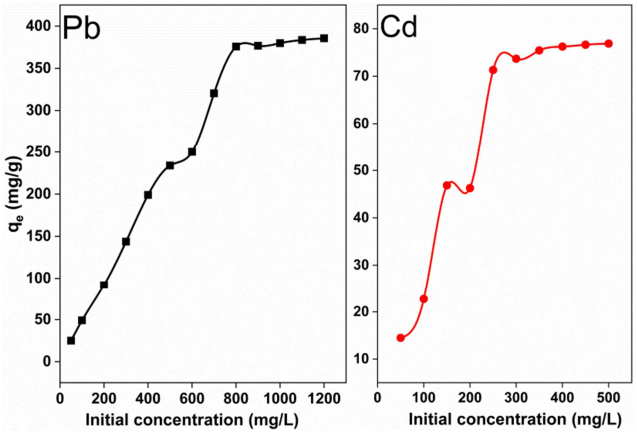

Figure 11. *The relation between adsorption capacity and initial concentration of Pb^{+2} and Cd^{+2}.*

In this context, two common isothermal models are used to explain the adsorption behavior of both Pb^{+2} and Cd^{+2} on faujasite. The first one is the Langmuir isothermal model herein, he postulated that there is no interaction between the adsorbate molecules on the surface of the adsorbent materials. Moreover, this adsorbent surface must be composed of a homogeneous infinity number of active sites that have similar energy values and on the whole only monolayer is formed [50, 51]. The linear equation of Langmuir is presented in Eq. (4).

$$C_e/q_e = 1/q_m b + C_e/q_m \quad (4)$$

Where C_e is the final concentration (mg/L), q_e is adsorbed heavy metals at equilibrium (mg/g), q_{max} is the maximum uptake capacity (mg/g), and b is the model isotherm constant (L/mg). Also, R_L parameter is calculated from Eq. (5).

$$R_L = 1/(1 + bC_o) \quad (5)$$

where b is previously defined and C_0 is the initial metal concentration. Where the R_L values are $0 \leq R_L \leq 1$. At R_L=0 the adsorption process proceeds reversibly and is favorable whereas at R_L = 1, the adsorption isotherm will take the linear form but at $R_L > 1$ the process is not favorable. All the parameters of this model are estimated and listed in Table 2. The linear plotting was represented in Figure 12. The obtained data reflect the following: (i) the adsorption of the two heavy metals could be described by this model where the correlation coefficient in the case of Pb^{+2} ($R^2 > 0.9$) while in Cd^{+2} (R^2 = 0.85) and (ii) RL values illustrate that the adsorption is favorable.

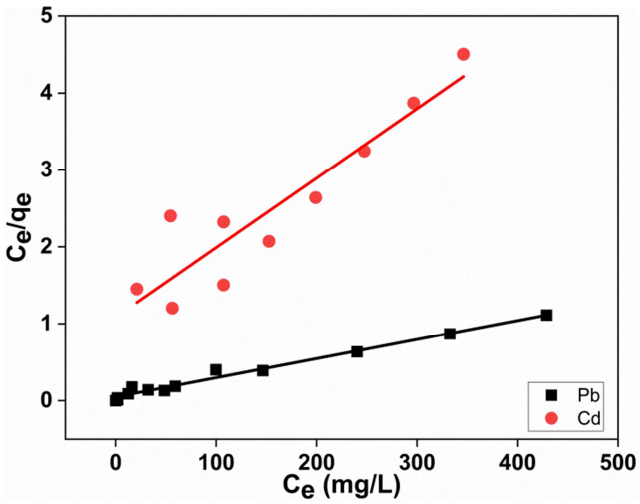

Figure 12. *The linear curves of the Langmuir model.*

Freundlich adsorption model represents the second one and it was postulated that the adsorption of heavy metals proceeded with the formation of multilayer and meanwhile the surface was heterogeneous [52]. The logarithmic form of this model is represented by equation (6).

$$\log q_e = \log k_f + 1/n \log C_e \quad (6)$$

Where k_f (L/g) is the model constant and 1/n is a constant that corresponds to the number of layers. Regarding the value of 1/n we have three different alternatives (i) when $0 < 1/n < 1$ the adsorption is favorable, (ii) at $1/n = 0$ adsorption will be irreversible, and (iii) at $1/n > 1$ the adsorption is not favorable. The parameters included in this model were obtained by plotting log q_e vs log c_e Figure 13 and are listed in Table 2. Checking the obtained adsorbed data upon applying such a model, one can conclude that the adsorption process of Pb^{+2} does not opay the model where the fitting possesses a poor correlation coefficient ($R^2 = 0.65$). Meanwhile, Cd^{+2} adsorption is as presentable fitting with $R^2 = 0.81$.

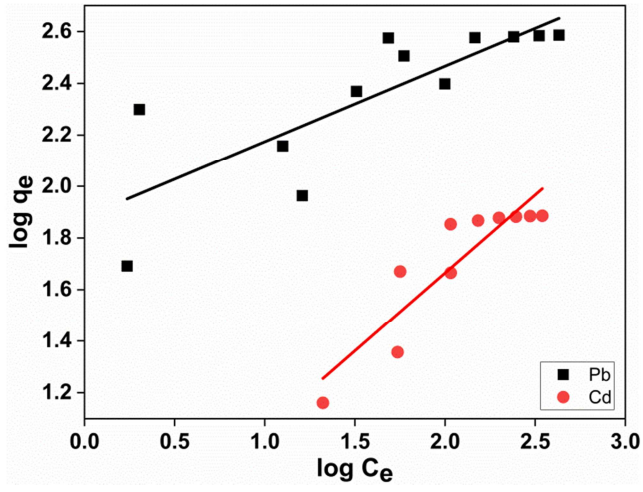

Figure 13. *The Fruindlich model.*

Table 2. *The estimated parameters of isothermal models.*

	parameters	Faujasite	
		Pb^{+2}	Cd^{+2}
Langmuir model	q_{max} (mg/g)	400	111.11
	b (L/mg)	0.0512	0.00828
	R^2	0.98	0.85
	R_L	0.023	0.376
Fruindlich model	1/n	0.2921	0.6043
	k_f	77.42	2.856
	R^2	0.65	0.81
Temkin model	B_T	56.643	24.823
	k_T	2.579	11.48
	R^2	0.71	0.83

4. Conclusion

Faujasite was synthesized from claystone as a precursor via hydrothermal processes. The synthetic material under investigation was used as an adsorbent for lead and cadmium ions from wastewater. The adsorbent material exhibits higher removal percentages amounting to 98% and 85% for Pb^{+2} and Cd^{+2} respectively. Also, it possesses higher capacities for the two adsorbate cations with values corresponding to 351 mg/g for Pb^{+2} and 97mg/g for Cd^{+2}. To suggest the mechanism of the adsorption process we apply some kinetic and isothermal models. Accordingly, our adsorption data were found to be fitted well with both pseudo-second-order ($R^2 > 0.9$) and Elovich ($R^2 > 0.9$ for Pb^{+2} and 0.86 for Cd^{+2}) as kinetic models. A trial was made to find the appropriate adsorption model that fits our adsorption data, we come to the conclusion that the Langmuir isothermal model has ($R^2 > 0.9$ for Pb^{+2} and 0.85 for Cd^{+2}). Though, we conclude that the adsorption process occurs through a chemisorption process via sharing and/or ion exchange at a heterogenous and energetic surface with the formation of a monolayer.

5. Recommendations

Faujasite, a low-cost alternative sorbent synthesized from claystone, has the potential to be used in heavy metal adsorption applications.

References

[1] V. N. Mehta, H. Basu, R. K. Singhal, S. K. Kailasa, Simple and sensitive colorimetric sensing of Cd^{2+} ion using chitosan dithiocarbamate functionalized gold nanoparticles as a probe, Sensors Actuators, B Chem. 220 (2015) 850–858. https://doi.org/10.1016/j.snb.2015.05.105.

[2] M. R. Abukhadra, F. M. Dardir, M. Shaban, E. A. Ahmed, M. F. Soliman, Superior removal of Co^{2+}, Cu^{2+} and Zn^{2+} contaminants from water utilizing spongy Ni/Fe carbonate–fluorapatite; preparation, application and mechanism, Ecotoxicol. Environ. Saf. 157 (2018) 358–368. https://doi.org/10.1016/j.ecoenv.2018.03.085.

[3] J. Sun, F. Yao, J. Wu, P. Zhang, W. Xu, Effect of nitrogen levels on photosynthetic parameters, morphological and chemical characters of saplings and trees in a temperate forest, J. For. Res. 29 (2018) 1481–1488. https://doi.org/10.1007/s11676-017-0547-8.

[4] V. N. Mehta, J. N. Solanki, S. K. Kailasa, Selective visual detection of Pb(II) ion via gold nanoparticles coated with a dithiocarbamate-modified 4′-aminobenzo-18-crown-6, Microchim. Acta. 181 (2014) 1905–1915. https://doi.org/10.1007/s00604-014-1287-5.

[5] S. Bhattacharjee, S. Chakrabarty, S. Maity, S. Kar, P. Thakur, G. Bhattacharyya, Removal of lead from contaminated water bodies using sea nodule as an adsorbent, Water Res. 37 (2003) 3954–3966. https://doi.org/10.1016/S0043-1354(03)00315-4.

[6] M. R. Abukhadra, B. M. Bakry, A. Adlii, S. M. Yakout, M. A. El-Zaidy, Facile conversion of kaolinite into clay nanotubes (KNTs) of enhanced adsorption properties for toxic heavy metals (Zn2+, Cd2+, Pb2+, and Cr6+) from water, J. Hazard. Mater. 374 (2019) 296–308. https://doi.org/10.1016/j.jhazmat.2019.04.047.

[7] D. Wang, X. Guan, F. Huang, S. Li, Y. Shen, J. Chen, H. Long, Removal of heavy metal ions by biogenic hydroxyapatite: Morphology influence and mechanism study, Russ. J. Phys. Chem. A. 90 (2016) 1557–1562. https://doi.org/10.1134/S0036024416080069.

[8] Y. Zhang, M. Xia, F. Wang, J. Ma, Experimental and theoretical study on the adsorption mechanism of Amino trimethylphosphate (ATMP) functionalized hydroxyapatite on Pb (II) and Cd (II), Colloids Surfaces A Physicochem. Eng. Asp. 626 (2021) 127029. https://doi.org/10.1016/j.colsurfa.2021.127029.

[9] N. Thi Thom, D. Thi Mai Thanh, P. Thi Nam, N. Thu Phuong, C. Buess-Herman, Adsorption behavior of Cd2+ ions using hydroxyapatite (HAp) powder, Green Process. Synth. 7 (2018) 409–416. https://doi.org/10.1515/gps-2018-0031.

[10] Y. Feng, Y. Wang, Y. Wang, S. Liu, J. Jiang, C. Cao, J. Yao, Simple fabrication of easy handling millimeter-sized porous attapulgite/polymer beads for heavy metal removal, J. Colloid Interface Sci. 502 (2017) 52–58. https://doi.org/10.1016/j.jcis.2017.04.086.

[11] A. Dąbrowski, Z. Hubicki, P. Podkościelny, E. Robens, Selective removal of the heavy metal ions from waters and industrial wastewaters by ion-exchange method, Chemosphere. 56 (2004) 91–106. https://doi.org/10.1016/j.chemosphere.2004.03.006.

[12] A. Bashir, L. A. Malik, S. Ahad, T. Manzoor, M. A. Bhat, G. N. Dar, A. H. Pandith, Removal of heavy metal ions from aqueous system by ion-exchange and biosorption methods, Environ. Chem. Lett. 17 (2019) 729–754. https://doi.org/10.1007/s10311-018-00828-y.

[13] B. Alyüz, S. Veli, Kinetics and equilibrium studies for the removal of nickel and zinc from aqueous solutions by ion exchange resins, J. Hazard. Mater. 167 (2009) 482–488. https://doi.org/10.1016/j.jhazmat.2009.01.006.

[14] M. M. Brbooti, B. a Abid, N. M. Al-shuwaiki, Removal of Heavy Metals Using Chemicals Precipitation, Enginering Technol. J. 29 (2011).

[15] S. Song, A. Lopez-Valdivieso, D. J. Hernandez-Campos, C. Peng, M. G. Monroy-Fernandez, I. Razo-Soto, Arsenic removal from high-arsenic water by enhanced coagulation with ferric ions and coarse calcite, Water Res. 40 (2006) 364–372. https://doi.org/10.1016/j.watres.2005.09.046.

[16] Q. Chen, Y. Yao, X. Li, J. Lu, J. Zhou, Z. Huang, Comparison of heavy metal removals from aqueous solutions by chemical precipitation and characteristics of precipitates, J. Water Process Eng. 26 (2018) 289–300. https://doi.org/10.1016/j.jwpe.2018.11.003.

[17] M. F. Hamid, N. Abdullah, N. Yusof, N. M. Ismail, A. F. Ismail, W. N. W. Salleh, J. Jaafar, F. Aziz, W. J. Lau, Effects of surface charge of thin-film composite membrane on copper (II) ion removal by using nanofiltration and forward osmosis process, J. Water Process Eng. 33 (2020). https://doi.org/10.1016/j.jwpe.2019.101032.

[18] N. Abdullah, N. Yusof, W. J. Lau, J. Jaafar, A. F. Ismail, Recent trends of heavy metal removal from water/wastewater by membrane technologies, J. Ind. Eng. Chem. 76 (2019) 17–38. https://doi.org/10.1016/j.jiec.2019.03.029.

[19] H. F. Shaalan, M. H. Sorour, S. R. Tewfik, Simulation and optimization of a membrane system for chromium recovery from tanning wastes, Desalination. 141 (2001) 315–324. https://doi.org/10.1016/S0011-9164(01)85008-6.

[20] M. Shi, H. Qiang, C. Chen, Z. Bano, F. Wang, M. Xia, W. Lei, Construction and evaluation of a novel three-electrode capacitive deionization system with high desalination performance, Sep. Purif. Technol. 273 (2021) 118976. https://doi.org/10.1016/j.seppur.2021.118976.

[21] D. Ozdes, C. Duran, H. B. Senturk, Adsorptive removal of Cd(II) and Pb(II) ions from aqueous solutions by using Turkish illitic clay, J. Environ. Manage. 92 (2011) 3082–3090. https://doi.org/10.1016/j.jenvman.2011.07.022.

[22] M. qin Jiang, X. ying Jin, X. Q. Lu, Z. liang Chen, Adsorption of Pb(II), Cd(II), Ni(II) and Cu(II) onto natural kaolinite clay, Desalination. 252 (2010) 33–39. https://doi.org/10.1016/j.desal.2009.11.005.

[23] N. R. E. RADWAN, M. HAGAR, K. CHAIEB, Adsorption of crystal violet dye on modified bentonites, Asian J. Chem. 28 (2016) 1643–1647. https://doi.org/10.14233/ajchem.2016.19725.

[24] M. M. Hussein, K. M. Khader, S. M. Musleh, Characterization of raw zeolite and surfactant-modified zeolite and their use in removal of selected organic pollutants from water, Int. J. Chem. Sci. 12 (2014) 815–844.

[25] D. Reinoso, M. Adrover, M. Pedernera, Green synthesis of nanocrystalline faujasite zeolite, Ultrason. Sonochem. 42 (2018) 303–309. https://doi.org/10.1016/j.ultsonch.2017.11.034.

[26] E. A. Abdelrahman, Synthesis of zeolite nanostructures from waste aluminum cans for efficient removal of malachite green dye from aqueous media, J. Mol. Liq. 253 (2018) 72–82. https://doi.org/10.1016/j.molliq.2018.01.038.

[27] E. A. Abdelrahman, D. A. Tolan, M. Y. Nassar, A Tunable Template-Assisted Hydrothermal Synthesis of Hydroxysodalite Zeolite Nanoparticles Using Various Aliphatic Organic Acids for the Removal of Zinc(II) Ions from Aqueous Media, J. Inorg. Organomet. Polym. Mater. 29 (2019) 229–247. https://doi.org/10.1007/s10904-018-0982-9.

[28] D. P. De-La-Vega, C. González, C. A. Escalante, J. Gallego, M. Salamanca, L. Manrique-Losada, Use of faujasite-type zeolite for ion adsorption in municipal wastewater, Tecnol. y Ciencias Del Agua. 9 (2018). https://doi.org/10.24850/j-tyca-2018-04-08.

[29] E. A. Abdelrahman, A. Alharbi, A. Subaihi, A. M. Hameed, M. A. Almutairi, F. K. Algethami, H. M. Youssef, Facile fabrication of novel analcime/sodium aluminum silicate hydrate and zeolite Y/faujasite mesoporous nanocomposites for efficient removal of Cu(II) and Pb(II) ions from aqueous media, J. Mater. Res. Technol. 9 (2020) 7900–7914. https://doi.org/10.1016/j.jmrt.2020.05.052.

[30] R. Shahrokhi-Shahraki, C. Benally, M. G. El-Din, J. Park, High efficiency removal of heavy metals using tire-derived activated carbon vs commercial activated carbon: Insights into the adsorption mechanisms, Chemosphere. 264 (2021) 128455. https://doi.org/10.1016/j.chemosphere.2020.128455.

[31] Z. Dong, F. Zhang, D. Wang, X. Liu, J. Jin, Polydopamine-mediated surface-functionalization of graphene oxide for heavy metal ions removal, J. Solid State Chem. 224 (2015) 88–93. https://doi.org/10.1016/j.jssc.2014.06.030.

[32] W. Zhan, L. Gao, X. Fu, S. H. Siyal, G. Sui, X. Yang, Green synthesis of amino-functionalized carbon nanotube-graphene hybrid aerogels for high performance heavy metal ions removal, Appl. Surf. Sci. 467–468 (2019) 1122–1133. https://doi.org/10.1016/j.apsusc.2018.10.248.

[33] L. Pivarčiová, O. Rosskopfová, M. Galamboš, P. Rajec, Adsorption behavior of Zn(II) ions on synthetic hydroxyapatite, Desalin. Water Treat. 55 (2015) 1825–1831. https://doi.org/10.1080/19443994.2014.927794.

[34] D. Zhu, L. Wang, D. Fan, N. Yan, S. Huang, S. Xu, P. Guo, M. Yang, J. Zhang, P. Tian, Z. Liu, A Bottom-Up Strategy for the Synthesis of Highly Siliceous Faujasite-Type Zeolite, Adv. Mater. 32 (2020) 1–7. https://doi.org/10.1002/adma.202000272.

[35] T. F. Chaves, H. O. Pastore, D. Cardoso, A simple synthesis procedure to prepare nanosized faujasite crystals, Microporous Mesoporous Mater. 161 (2012) 67–75. https://doi.org/10.1016/j.micromeso.2012.05.022.

[36] E. A. Abdelrahman, R. M. Hegazey, Utilization of waste aluminum cans in the fabrication of hydroxysodalite nanoparticles and their chitosan biopolymer composites for the removal of Ni(II) and Pb(II) ions from aqueous solutions: Kinetic, equilibrium, and reusability studies, Microchem. J. 145 (2019) 18–25. https://doi.org/10.1016/j.microc.2018.10.016.

[37] M. R. Abukhadra, M. Mostafa, Effective decontamination of phosphate and ammonium utilizing novel muscovite/phillipsite composite; equilibrium investigation and realistic application, Sci. Total Environ. 667 (2019) 101–111. https://doi.org/10.1016/j.scitotenv.2019.02.362.

[38] S. Çoruh, The removal of zinc ions by natural and conditioned clinoptilolites, Desalination. 225 (2008) 41–57. https://doi.org/10.1016/j.desal.2007.06.015.

[39] H. K. Boparai, M. Joseph, D. M. O'Carroll, Kinetics and thermodynamics of cadmium ion removal by adsorption onto nano zerovalent iron particles, J. Hazard. Mater. 186 (2011) 458–465. https://doi.org/10.1016/j.jhazmat.2010.11.029.

[40] D. Ozdes, A. Gundogdu, B. Kemer, C. Duran, H. B. Senturk, M. Soylak, Removal of Pb(II) ions from aqueous solution by a waste mud from copper mine industry: Equilibrium, kinetic and thermodynamic study, J. Hazard. Mater. 166 (2009) 1480–1487. https://doi.org/10.1016/j.jhazmat.2008.12.073.

[41] A. M. Anielak, R. Schmidt, Sorption of lead and cadmium cations on natural and manganese-modified zeolite, Polish J. Environ. Stud. 20 (2011) 15–19.

[42] J. A. Abudaia, M. O. Sulyman, K. Y. Elazaby, S. M. Ben-Ali, Adsorption of Pb (II) and Cu (II) from Aqueous Solution onto Activated Carbon Prepared from Dates Stones, Int. J. Environ. Sci. Dev. 4 (2013) 191–195. https://doi.org/10.7763/ijesd.2013.v4.333.

[43] K. Y. Foo, B. H. Hameed, Preparation, characterization and evaluation of adsorptive properties of orange peel based activated carbon via microwave induced K 2CO 3 activation, Bioresour. Technol. 104 (2012) 679–686. https://doi.org/10.1016/j.biortech.2011.10.005.

[44] A. Villabona-Ortíz, Á. González-Delgado, C. Tejada-Tovar, Equilibrium, Kinetics and Thermodynamics of Chromium (VI) Adsorption on Inert Biomasses of Dioscorea rotundata and Elaeis guineensis, Water (Switzerland). 14 (2022). https://doi.org/10.3390/w14060844.

[45] U. Khalil, M. B. Shakoor, S. Ali, S. R. Ahmad, M. Rizwan, A. A. Alsahli, M. N. Alyemeni, Selective removal of hexavalent chromium from wastewater by rice husk: Kinetic, isotherm and spectroscopic investigation, Water (Switzerland). 13 (2021). https://doi.org/10.3390/w13030263.

[46] A. Q. Alorabi, F. A. Alharthi, M. Azizi, N. Al-Zaqri, A. El-Marghany, K. A. Abdelshafeek, Removal of lead(Ii) from synthetic wastewater by lavandula pubescens decne biosorbent: Insight into composition–adsorption relationship, Appl. Sci. 10 (2020) 1–16. https://doi.org/10.3390/app10217450.

[47] M. Manjuladevi, R. Anitha, S. Manonmani, Kinetic study on adsorption of Cr(VI), Ni(II), Cd(II) and Pb(II) ions from aqueous solutions using activated carbon prepared from Cucumis melo peel, Appl. Water Sci. 8 (2018) 1–8. https://doi.org/10.1007/s13201-018-0674-1.

[48] R. Katal, M. S. Baei, H. T. Rahmati, H. Esfandian, Kinetic, isotherm and thermodynamic study of nitrate adsorption from aqueous solution using modified rice husk, J. Ind. Eng. Chem. 18 (2012) 295–302. https://doi.org/10.1016/j.jiec.2011.11.035.

[49] A. E. A. Said, A. A. M. Aly, M. N. Goda, M. A. El-Aal, M. Abdelazim, Adsorptive Remediation of Congo Red Dye in Aqueous Solutions Using Acid Pretreated Sugarcane Bagasse, J. Polym. Environ. 28 (2020) 1129–1137. https://doi.org/10.1007/s10924-020-01665-3.

[50] A. E.-A. A. Said, M. N. Goda, Superior Competitive Adsorption Capacity of Natural Bentonite in the Efficient Removal of Basic Dyes from Aqueous Solutions, ChemistrySelect. 6 (2021) 2790–2803. https://doi.org/10.1002/slct.202100575.

[51] A. H. Swenson, N. P. Stadie, Stadie_Langmuir_2019_FINAL.pdf, 16 (2019) 5409–5426. https://doi.org/10.1021/acs.langmuir.9b00154.Made.

[52] E. D. Asuquo, A. D. Martin, Sorption of cadmium (II) ion from aqueous solution onto sweet potato (Ipomoea batatas L.) peel adsorbent: Characterisation, kinetic and isotherm studies, J. Environ. Chem. Eng. 4 (2016) 4207–4228. https://doi.org/10.1016/j.jece.2016.09.024.